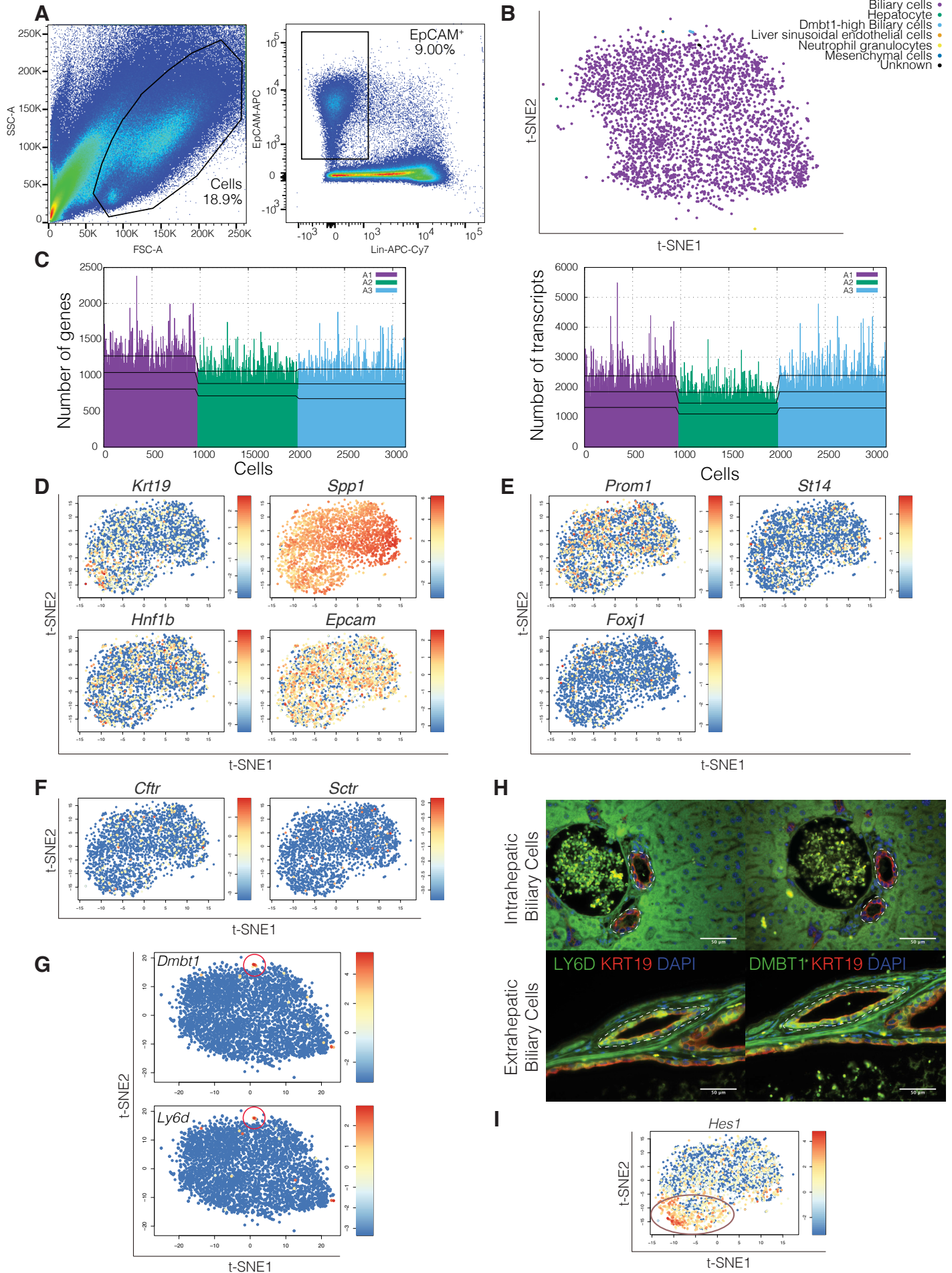# Figure S1

Figure S1. Extended Analysis of ScRNA-Seq Data for BECs, Related to Figure 1.

(**A**) Gating strategy for isolation of BECs by FACS. BECs were sorted on forward scatter (FSC) and side scatter (SSC) and subsequently by EpCAM$^+$, Lin$^-$ (CD11b, CD45, TER119) and DAPI$^-$. Approximately 1500 cells per sample were encapsulated with the inDrops platform and analyzed by next generation sequencing.

(**B**) t-SNE plot of all three combined homeostatic BEC samples identifying non-biliary cells by different colors, which were subsequently excluded from further analysis.

(**C**) Histograms showing number of annotated genes per cell (Left) and number of transcripts per cell (Right) across three adult homeostatic BEC scRNA-seq samples. Different libraries are indicated in different colors. The black horizontal lines indicate the mean ± SD for each library.

(**D**) t-SNE plots showing expression in log2 scale of the common biliary markers *Krt19*, *Spp1*, *Hnf1b*, and *Epcam*.

(**E**) Expression of the previously proposed biliary progenitor markers *Prom1, St14,* and *Foxj1*, as represented by t-SNE.

(**F**) t-SNE plots of genes previously found to correlate with large, distal BECs, *Cftr* and *Sctr*. Colors denote relative expression of respective gene in each cell.
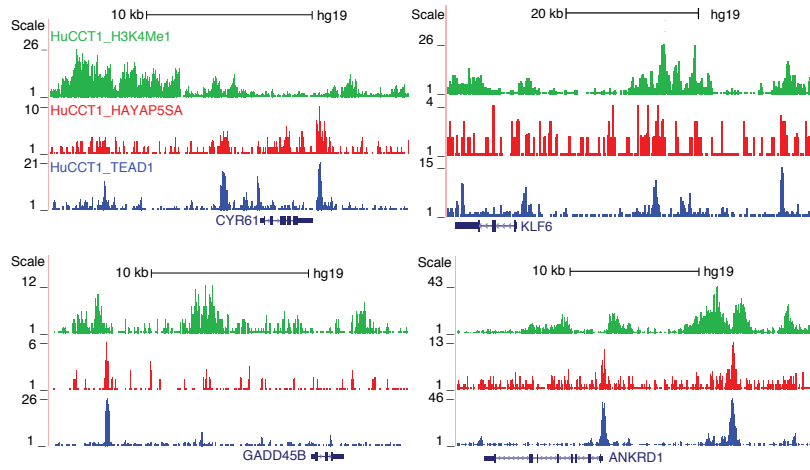
(**G**) Identification of a populations of extrahepatic biliary cells marked by *Dmbt1* and *Ly6d* expression, as represented by t-SNE. Red circle highlights a small cluster of cells identified by RaceID3 that highly co-express *Dmbt1* and *Ly6d*.

(**H**) IF for LY6D/KRT19/DAPI and DMBT1/KRT19/DAPI in intrahepatic and extrahepatic BECs. Positive DMBT1 and LY6D signal is only observed in extrahepatic BECs.
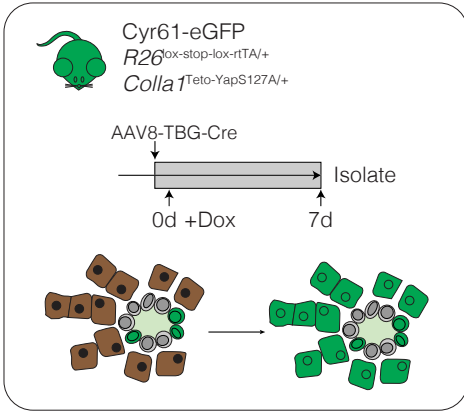
(**I**) t-SNE plot showing expression in log2 scale of *Hes1*. Colors denote relative expression of respective gene in each cell.
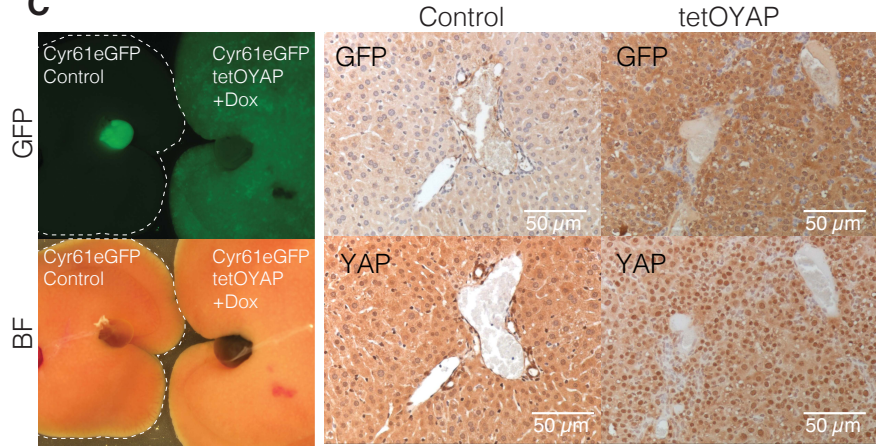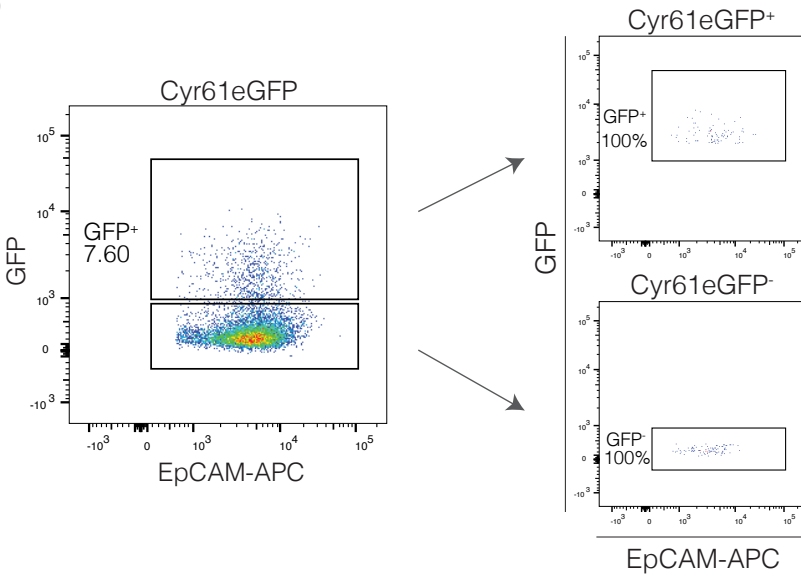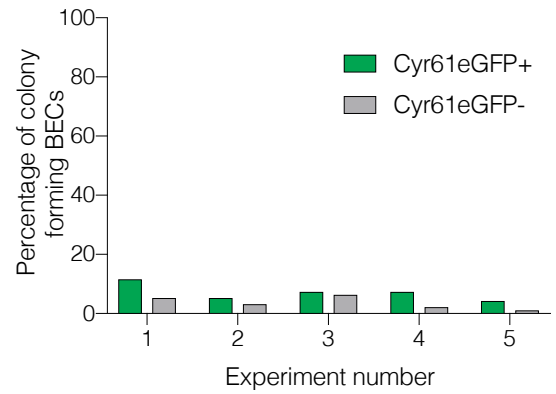
Figure S2

A

B

Cyr61-eGFP
$R26^{\text{lox-stop-lox-rtTA/+}}$
$Col1a1^{\text{Teto-YapS127A/+}}$

AAV8-TBG-Cre

Isolate
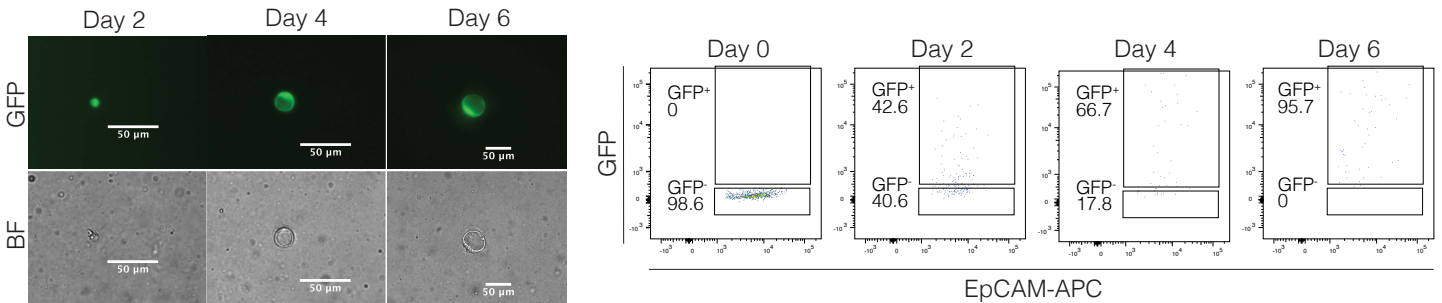
0d +Dox   7d

C

Control   tetOYAP

D

E

F

Figure S2. Genomic Tracks of ChIP-seq Data and Supplementary Data for Cyr61eGFP Mouse Experiments, **Related to Figure 2.**

(**A**) Genomic tracks displaying ChIP-seq data for YAP^{5SA} (constitutively-active YAP), TEAD1, and H3K4Me1 in a human liver cholangiocarcinoma cell line, HuCCT1, around the genomic location of genes *CYR61*, *GADD45B*, *KLF6*, and *ANKRD1* identified by scRNA-seq as associated with YAP activity.
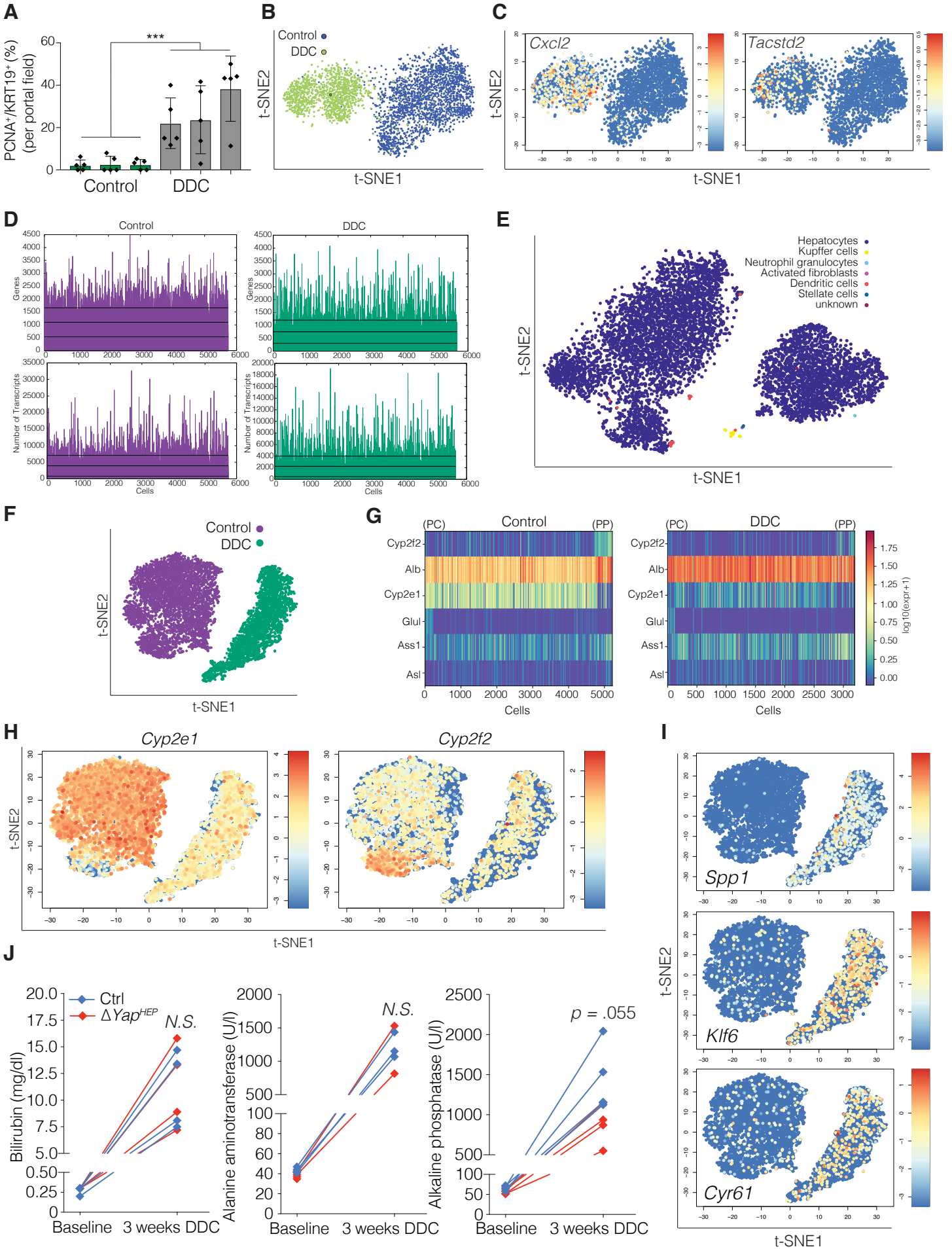
(**B**) Schematic showing genetic mouse model used to examine Cyr61eGFP YAP responsiveness *in vivo*. Cyr61eGFP mice were crossed to *TetOYap* mice (*R26*$^{lox-stop-lox-rtTA/+}$; *Col1a1*$^{tetO-YapS127A/+}$), which allows for doxycycline inducible expression of constitutively active, YAP^{S127A}. These mice were administered AAV8.TBG.PI.Cre.rBG (AAV-Cre) at a dose of 1x10^11 GC and given doxycycline for 1 week to overexpress of YAP^{S127A} specifically in hepatocytes.

(**C**) Left: Fluorescence and bright field images confirm upregulation of GFP in CYR61eGFP*; TetOYAP* mouse livers as a surrogate for active YAP overexpression upon doxycycline administration compared to control. The bright fluorescent spot in the CYR61eGFP only mouse represents the gallbladder containing fluorescent bile. This is not seen in the *TetOYAP* mouse liver, where bile usually assumes a darker color. Right: IHC of serial sections for GFP, YAP, and pCK in Cyr61eGFP and Cyr61eGFP; *TetOYAP* livers. Active, nuclear YAP is visible in *TetOYap* livers with concurrent GFP upregulation.

(**D**) FACS plot of EpCAM$^+$ BECs from Cyr61eGFP mouse livers which were sorted into GFP$^-$ and GFP$^+$ populations and plated each in a 96-well plate at a single cell per well. Purity was confirmed in a double sort as indicated in the additional FACS plots.

(**E**) Bar plot showing percentage of wells that contained colonies 14 days after seeding (n=5 replicative experiments).

(**F**) Left: Representative fluorescent and bright field images of biliary organoids sorted from EpCAM$^+$ GFP$^-$ cells from Cyr61eGFP mouse livers at the indicated time points after seeding. Right: Representative FACS plots of originally 5000 GFP$^-$ BECs sorted into each organoid well and monitored by FACS for GFP expression at 2 days, 4 days, and 6 days after plating.

Figure S3

A PCNA+/KRT19+ (%) (per portal field) — Control, DDC — ***

B t-SNE2 vs t-SNE1 — Control, DDC

C *Cxcl2*, *Tacstd2* — t-SNE2 vs t-SNE1

D Control, DDC — Genes, Number of Transcripts vs Cells

E t-SNE2 vs t-SNE1 — Hepatocytes, Kupffer cells, Neutrophil granulocytes, Activated fibroblasts, Dendritic cells, Stellate cells, unknown

F t-SNE2 vs t-SNE1 — Control, DDC

G (PC) Control (PP), (PC) DDC (PP) — Cyp2f2, Alb, Cyp2e1, Glul, Ass1, Asl — log10(expr+1)

H *Cyp2e1*, *Cyp2f2* — t-SNE2 vs t-SNE1

I *Spp1*, *Klf6*, *Cyr61* — t-SNE2 vs t-SNE1

J Bilirubin (mg/dl), Alanine aminotransferase (U/l), Alkaline phosphatase (U/l) vs Baseline, 3 weeks DDC — Ctrl, ΔYap^{HEP} — N.S., N.S., $p = .055$

Figure S3. **Extended Data From scRNA-seq Analyses of DDC-Injured BECs and Hepatocytes, Related to Figures 3 and 4.**

(**A**) Bar-scatter plot indicating the number of PCNA+ BECs assessed by IF of mice fed with standard or DDC-supplemented feed for 1 week. Data are mean ± SD of 5 portal fields per mouse (n = 3 mice per group).

(**B**) t-SNE plot comparing scRNA-seq data from homeostatic (**Figure 1C**) (blue) and DDC-injured BECs (green).

(**C**) Expression of *Cxcl2* and *Tacstd2*, two well-known upregulated genes upon DDC injury, as represented by t-SNE. Colors denote relative expression of respective gene in each cell (log2 scale).

(**D**) Histograms showing number of transcripts per cell and number of annotated genes per cell across homeostatic and DDC-injured hepatocytes from the scRNA-seq samples. The black horizontal lines indicate the mean and mean plus/minus standard deviation for each library.

(**E**) t-SNE plot of combined hepatocyte samples (control and DDC) identifying non-biliary cells by different colors, which were subsequently excluded from further analysis.

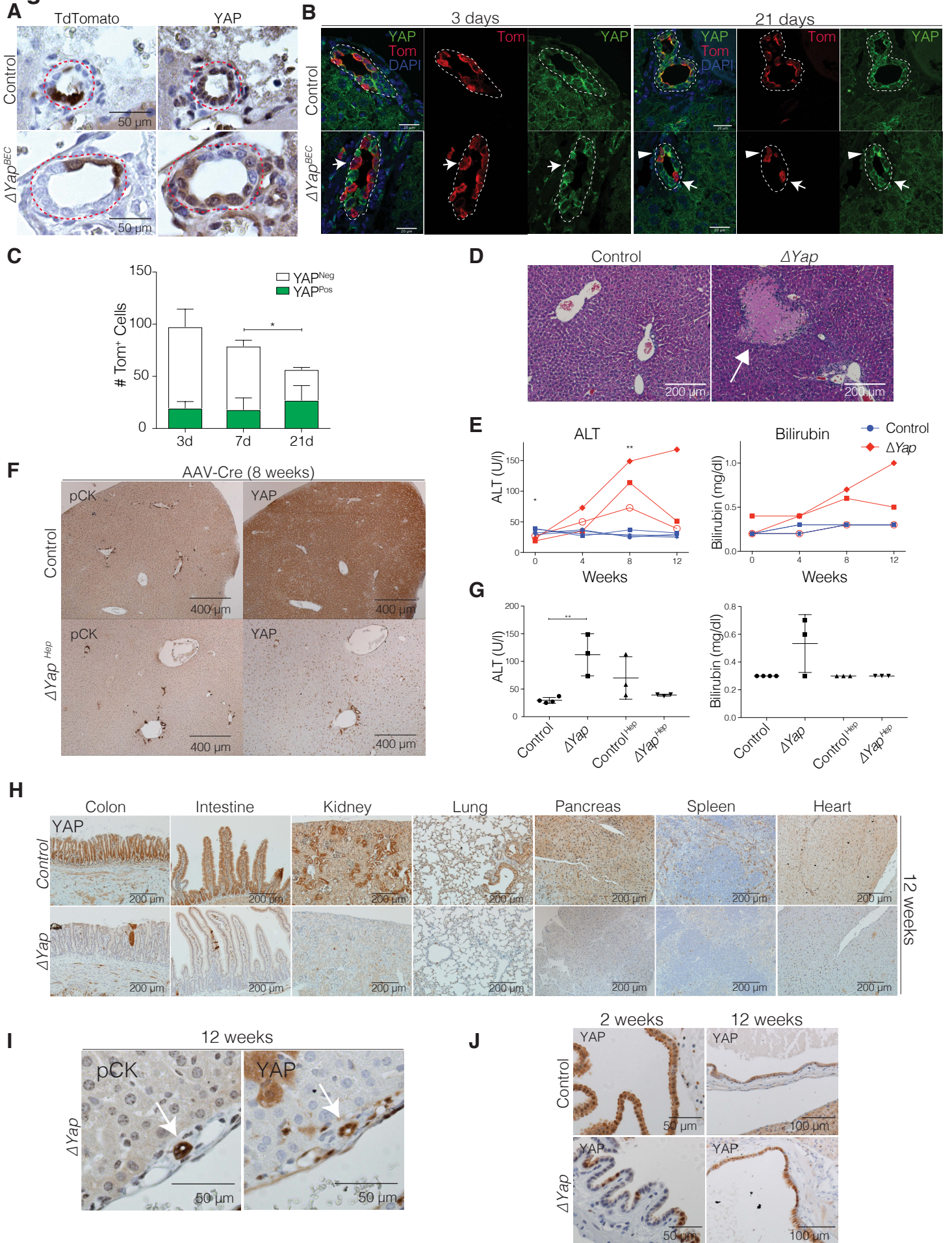(**F**) t-SNE plot of scRNA-seq data comparing homeostatic (purple) and DDC-injured hepatocytes (green).

(**G**) Heatmap of landmark zonation genes evaluated according to the algorithm of Halpern et al.(Halpern et al., 2017) for single hepatocytes isolated from homeostatic and DDC injured livers. Colors denote normalized expression in log 10 scale of respective gene in each cell. Cells in the x axis are ordered according to relative distance to the pericentral (PC) vein area (left) and the periportal (PP) area (right).

(**H**) Normalized expression in log2 scale of two well-known hepatocyte zonation genes *Cyp2e1* and *Cyp2f2* as represented by t-SNE of the merged hepatocyte samples (control left, DDC right).

(**I**) Normalized expression (in log2 scale) of the ductal marker *Spp1* and of two YAP target genes, *Cyr61* and *Klf6* as represented by t-SNE.

(**J**) Timeline of blood chemistry analysis of ΔYap^{HEP} mice and controls at baseline and 3 weeks after DDC diet for bilirubin, alanine aminotransferase (ALT) and alkaline phosphatase (n = 4 mice per group).

Figure S4

A
TdTomato | YAP
Control
ΔYap^{BEC}
50 µm

B 3 days | 21 days
YAP Tom DAPI | Tom | YAP | YAP Tom DAPI | Tom | YAP
Control
ΔYap^{BEC}

C
Tom⁺ Cells
YAP^{Neg}
YAP^{Pos}
*
3d 7d 21d

D Control | ΔYap
200 µm

E ALT | Bilirubin
Control
ΔYap
ALT (U/l) | Bilirubin (mg/dl)
* | **
Weeks | Weeks

F AAV-Cre (8 weeks)
pCK | YAP
Control
ΔYap^{Hep}
400 µm

G
ALT (U/l) | Bilirubin (mg/dl)
**
Control ΔYap Control^{Hep} ΔYap^{Hep}

H Colon | Intestine | Kidney | Lung | Pancreas | Spleen | Heart
YAP
Control
ΔYap
200 µm (each) | 12 weeks

I 12 weeks
pCK | YAP
ΔYap
50 µm

J 2 weeks | 12 weeks
YAP | YAP
Control
ΔYap
50 µm | 100 µm

Figure S4. Effects of Inducible *Yap* KO in BECs, Hepatocytes and All Cells, Related to Figure 5.
(**A**) Immunostaining for Tom and YAP in serial liver sections depicting bile ducts from ΔYap^{BEC} and Control mice, 3 days after TAM, demonstrating average *Yap* KO efficiency of ~40%. Dashed lines outline bile ducts.

(**B**) IF of YAP and Tom, at the indicated time points after *Yap* KO. Arrows indicate Tom$^+$ YAP$^-$ cells. Arrowheads illustrate escaper YAP$^+$ Tom$^+$ cells at 21 days. Dashed lines highlight bile ducts.

(**C**) Bar plot illustrating the absolute number of YAP$^+$ and YAP$^-$ cells within the Tom$^+$ cell population. A decrease in the total number of YAP$^-$ cells over time is observed. Data are mean ± SD for 10 portal areas of 2 mice per group.

(**D**) Low magnification H&E images of ΔYap livers 12 weeks after start with Dox. Arrows indicate patches of necrosis.

(**E**) Serial blood chemistry analysis for alanine aminotransferase (ALT) and bilirubin levels of ΔYap and Control mice at the designated weeks after start of Dox (n = 3 mice per group). Each line represents a mouse.

(**F**) Immunostains for pCK and YAP 8 weeks after administration of AAV-Cre (1x10^11 GC) to *Yap$^{fl/fl}$*; R26$^{LSL\text{-}TdTomato/+}$ (ΔYap^{Hep}) and R26$^{LSL\text{-}TdTomato/+}$ (Control^{Hep}) control mice without observable biological differences.

(**G**) Blood chemistry analysis (bilirubin and ALT) for ΔYap^{Hep}, ΔYap, and control mice 8 weeks after recombination. Data are mean ± SD with each symbol representing a mouse.

(**H**) Immunostains for YAP of indicated tissues from ΔYap and Control mice 12 weeks after Dox. No pathological morphology was observed in H&E stains of the selected tissues.

(**I**) Serial immunostains for pCK and YAP of a portal field from a ΔYap mouse showing escaper YAP$^+$ BECs (arrows) at the 12-week time point after the start of Dox.

(**J**) Representative immunostains for YAP from gallbladder in ΔYap and control mice 2 and 12 weeks after start of Dox, indicating significant repopulation by Yap+ escaper cells over time.

Figure S5
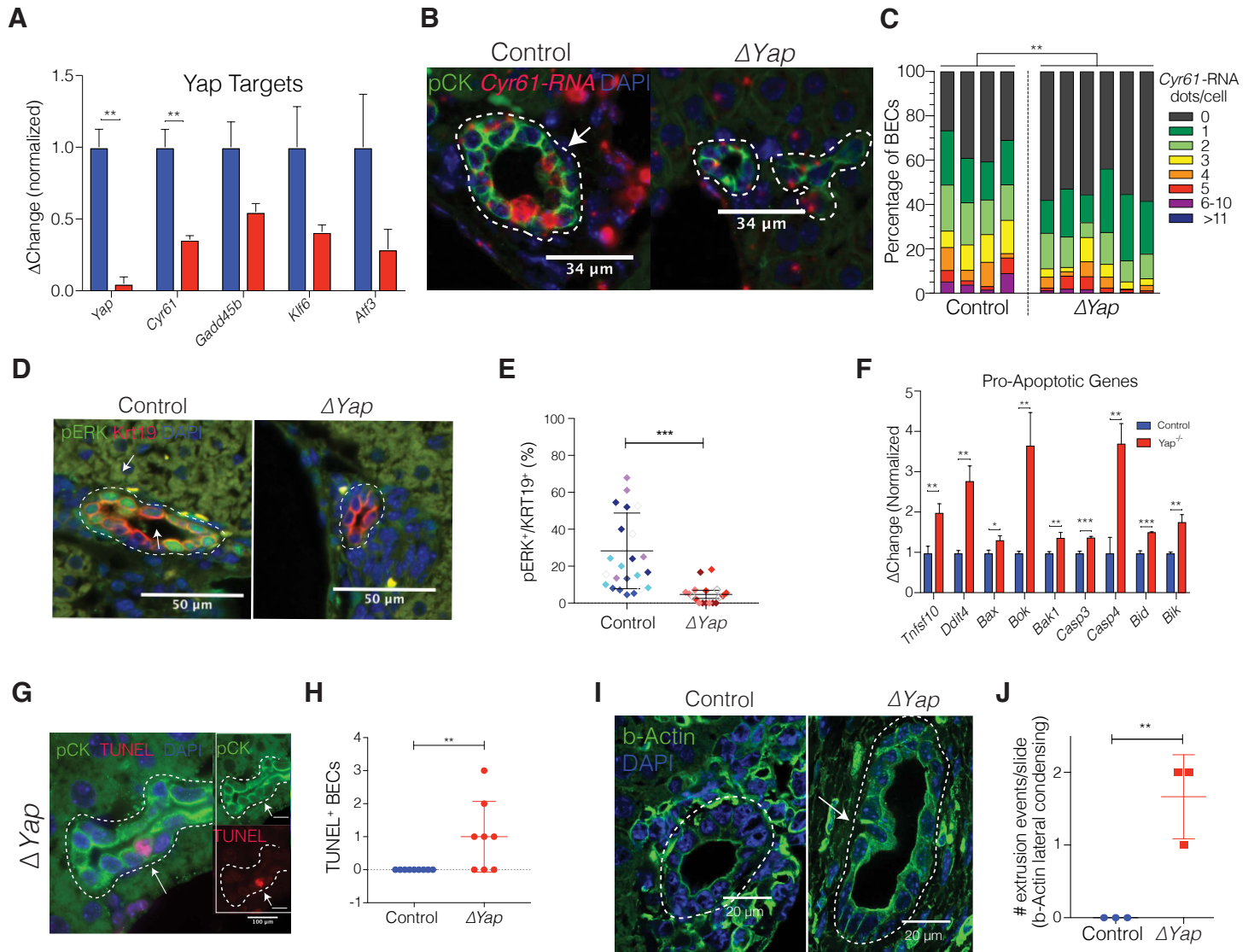
Figure S5. Evaluation of the transcriptional changes upon *Yap* KO in BECs and Cell Death, Related to Figure 5.

(**A**) qRT-PCR of bulk RNA from sorted BECs from Δ*Yap* and control mice. Data are mean ± SD (n = 3 mice per group).

(**B**) RNA-ISH for Cyr61 and co-stained for pCK from Δ*Yap* and Control mice 2 weeks after the start of Dox. Dotted lines highlight bile ducts. Arrow indicates BEC with high counts of *Cyr61* RNA molecules.

(**C**) Distribution bar plot of *Cyr61*-RNA ISH quantification for Δ*Yap* and Control mice 2 weeks after the start of Dox. Each bar represents a mouse, and BECs are color-coded according to the contained number of *Cyr61*-RNA and shown as percentage of cumulative 6 portal fields counted. P-values were computed using the Kullback-Leibler test.

(**D**) IF of pERK and KRT19 of Δ*Yap* and Control mice 2 weeks after the start of Dox. Dotted lines highlight bile ducts and arrows indicate pERK-positive cells.

(**E**) Quantification of the ratio of pERK$^+$ cells per total number of KRT19$^+$ cells. Each diamond represents a portal field counted, different colors denote each mouse (5 portal fields per mouse). Indicated are mean ± SD for three biological replicates.

(**F**) Fold change of RNA sequencing data of pro-apoptotic genes from BECs upon *Yap* KO. Data are mean ± SD (n = 3 per group).

(**G**) IF for pCK and TUNEL assay depicting a bile duct in a Δ*Yap* mouse 2 weeks after doxycycline administration. Dotted lines highlight bile ducts and arrow illustrates TUNEL$^+$ cell.

(**H**) The total number of TUNEL$^+$ cells in each portal field per liver section. Data are mean ± SD with each dot representing a mouse (n = 9 control, n = 8 Δ*Yap*).

(**I**) IF for ß-Actin on Δ*Yap* and Control mice show basal actin condensation in a single cell upon *Yap* KO, typical of cellular extrusion. Dotted lines highlight bile ducts and arrow points to extruding cell in Δ*Yap* sample.

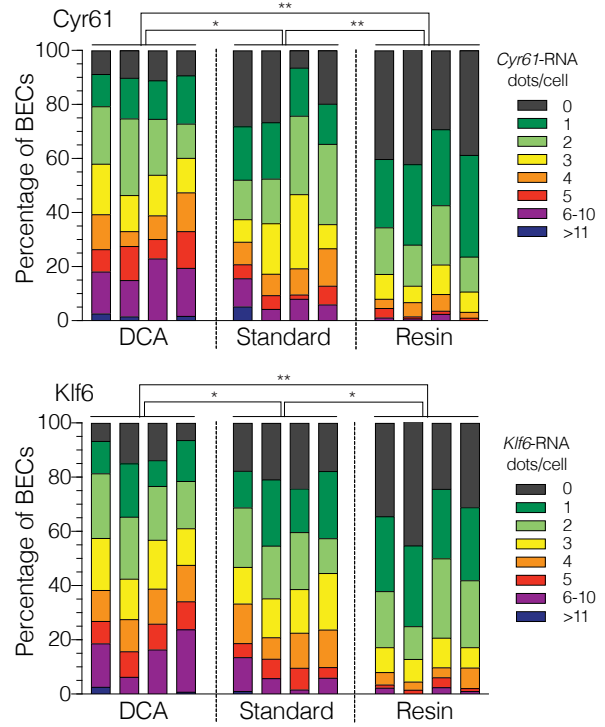(**J**) Quantification of the number of extruding BECs per section. Data are mean ± SD (n = 3 mice per group).

Figure S6

A

B

C

Intrahepatic bile duct

Gallbladder
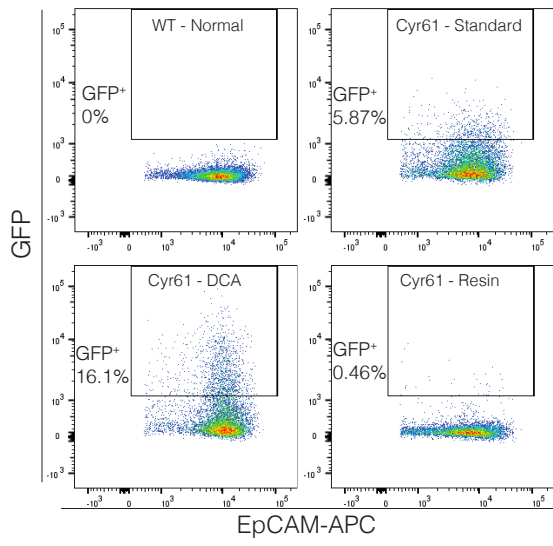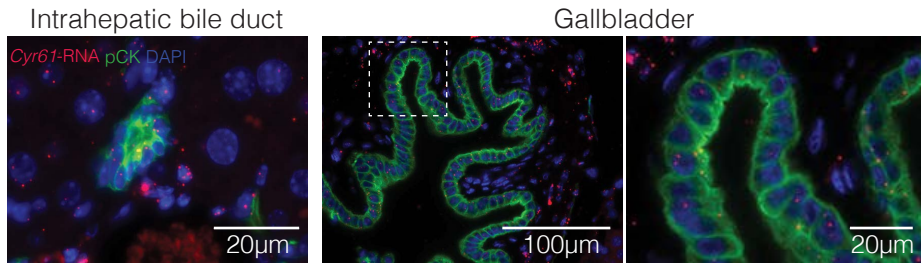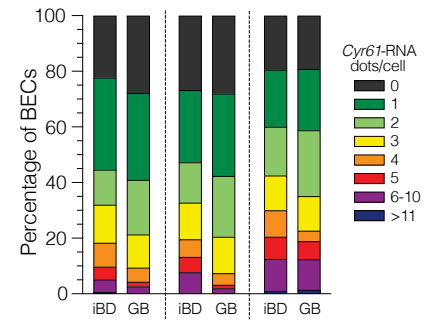
D

Figure S6. Effect of BA Modulation on YAP-Target Gene Expression, Related to Figure 6.

(**A**) FACS analysis of isolated EpCAM$^+$ BECs from C57Bl/6J (WT) mice administered standard feed and Cyr61eGFP (Cyr61) mice administered standard, DCA, or resin feed, indicating percentage of GFP$^+$ cells.

(**B**) Distribution bar plot of *Cyr61*-RNA and *Klf6*-RNA ISH quantification from **Figure 6E** for the indicated groups. Each bar represents a mouse, and BECs are color-coded according to the contained number of *Cyr61*-RNA and shown as percentage of cumulative 5 portal fields counted. P-values were computed using the Kullback-Leibler test.

(**C**) Representative images of RNA-ISH for *Cyr61* and co-stained for pCK from intrahepatic bile ducts and gallbladder.

(**D**) Distribution bar plot of *Cyr61*-RNA ISH quantification of paired intratepatic bile ducts (iBD) and gallbladder (GB) from 3 different mice. BECs are color-coded according to the contained number of *Cyr61*-RNA and shown as percentage of cumulative 5 200X images counted. P-values were computed using the Kullback-Leibler test and were not significant between iBD and GB.
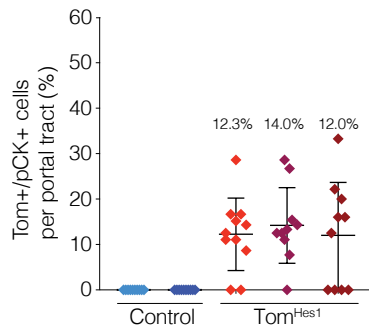
Figure S7

A

B

Cells with ≥ 3 unique transcripts

C

YAP active cells   YAP inactive cells

Abcb1a   *Abcc3*   *Slc10a2*

Slc4a2   *Muc1*   *Iqgap1*

Transcripts (UMI)

D

N.S

Control   *Tgr5* KO

E

N.S

Control   *Iqgap1* KO

Cyr61-RNA
dots/cell

0
1
2
3
4
5
6-10
> 11
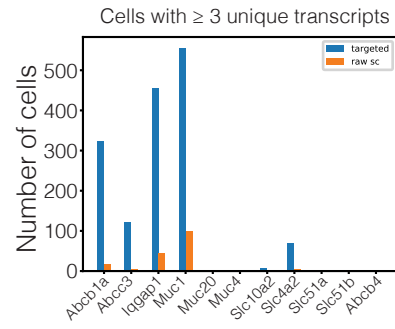
Figure S7. Targeted scRNA-seq Analysis and Evaluation of *Tgr5* and *Iqgap1* KO on YAP targets in BECs, Related to Figure 7.

(**A**) Scatter plot of the quantification of Tom$^+$ BECs per portal tract in Hes1$^{CreERT2/+}$; *R26*$^{LSL\text{-}TdTomato/+}$ mice (Tom^{Hes1}, n = 3) and *R26*$^{LSL\text{-}TdTomato/+}$ (Control, n = 2), 5 days after administration of 1mg TAM i.p. Each diamond represents a portal tract, indicated are mean ± SD, and average percentage per mouse.

(**B**) Bar plot depicting the number of cells from the merged control BEC scRNA-seq (Figure 1) containing at least 3 or more unique transcripts for the respective gene in the primary data set (orange) and after targeted amplification (blue). For further information about the selected genes, see **Table S6**.

(**C**) Histogram of the successfully amplified transcripts from the control BEC scRNA-seq libraries, showing the frequency of cells (y-axis) containing a certain number of unique transcripts (x-axis). Cells are stratified according to their YAP activity as defined in Figure 1, with orange indicating YAP-active cells and blue YAP-inactive cells. No significant differences in expression between the two groups can be observed, and statistical evaluation with Kolmogorov-Smirnov test did not indicate significance for any gene.

(**D**) Distribution bar plot of *Cyr61*-RNA ISH quantification for *Tgr5* KO and Control. Each bar represents a mouse. BECs are color-coded according to the contained number of *Cyr61*-RNA dots and shown as percentage of cumulative 10 portal fields counted. P-values were computed using the Kullback-Leibler test.
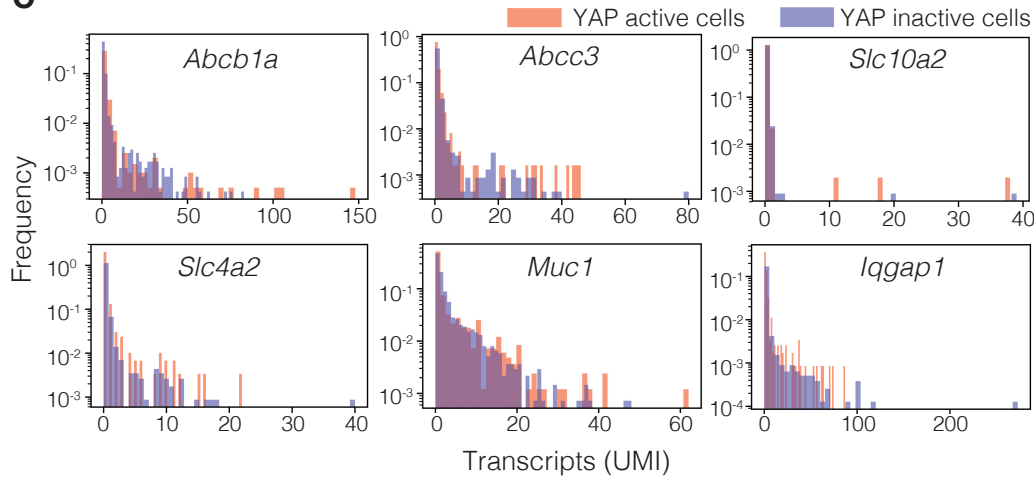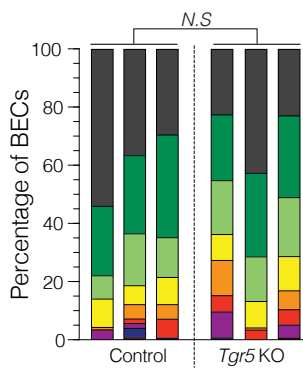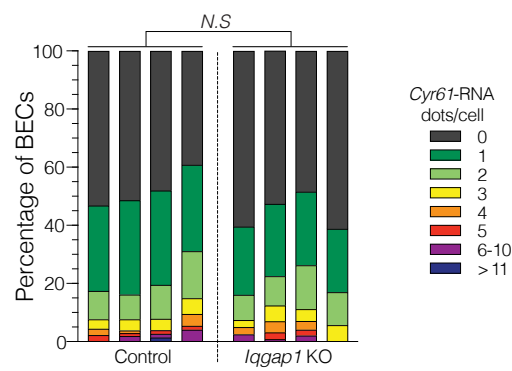
(**E**) Distribution bar plot of *Cyr61*-RNA ISH quantification for *Iqgap1* KO and Control. Each bar represents a mouse. BECs are color-coded according to the contained number of *Cyr61*-RNA dots and shown as percentage of cumulative 10 portal fields counted. P-values were computed using the Kullback-Leibler test.

Table S2. Genes which define Dmbt1 cluster analysis from scRNA-seq of homeostatic BECs, Related to Figure 1.

Gene Symbol	Mean.ncl	Mean.cl	Fold Change	p-value
Dmbt1	0.1223	24.3249	198.9246	< 2.2E-308
S100a6	0.2392	7.3451	30.7031	2.12E-10
Spink4	0.0908	1.3592	14.9686	0.00388
Ly6d	0.0964	1.3862	14.3785	0.00436
Sfn	0.1273	1.6667	13.0943	0.00744
Plaur	0.1212	1.1800	9.7368	0.00677
Itpkc	0.1314	1.2363	9.4089	0.00791
Tff2	0.2073	1.9164	9.2433	0.01873
Crip1	0.2671	2.2153	8.2952	0.00260
Epha2	0.1747	1.1910	6.8164	0.01359
Wfdc2	0.2827	1.6769	5.9320	0.03314
F3	0.3367	1.8754	5.5697	0.04540
Krt19	0.3157	1.2966	4.1066	0.04047
Cox17	0.3087	1.2236	3.9636	0.03886
Rps23	0.7684	2.4225	3.1527	0.04293
Rn45s	0.7807	2.4416	3.1275	0.04463
Fosb	0.3400	1.0044	2.9546	0.04618
Jund	0.7379	2.0305	2.7517	0.03887
Rps21	1.6381	4.4879	2.7397	0.02577
Ifrd1	0.7638	2.0095	2.6309	0.04230
Rpl41	2.7767	6.4499	2.3229	0.02336
Hspa8	3.1836	0.5187	0.1629	0.04136
Spp1	17.4675	2.0591	0.1179	4.20E-06
Hspa1b	6.7499	0.6337	0.0939	0.00116
Hspa1a	4.1376	0.2009	0.0486	0.01591
Anxa5	3.4001	0.0860	0.0253	0.03330
Alb	4.4723	0.0860	0.0192	0.01138
Apoe	11.0453	0.0860	0.0078	1.55E-05

Table S6. List of Genes Selected for Targeted Amplification from scRNA-seq libraries, Related to Figure 7.

Gene ID	Alias	Function	Amplification
Transporters			
Slc10a2	Asbt	Main apical BA transporter	
Slc4a2	AE2	Main apical bicarbonate exporter	
Abcb4	Mdr2	Basolaterally expressed BA transporter, associated with genetic cholestasis	Unsuccessful
Abcb1a	MDR/TAP	Member of MDR/TAP subfamily, basolateral efflux pump of modified BAs and xenobiotics	
Slc51a	Osta	Basolaterally expressed heteromeric Osta-Ostb exporter	Unsuccessful
Slc51b	Ostb	Basolaterally expressed heteromeric Osta-Ostb exporter	Unsuccessful
Abcc3	Mrp3	Involved in basolateral BA efflux, expression induced in cholestasis	
Receptors			
Iqgap1		BA induce Iqgap1 expression which in turn upregulates Yap in hepatocytes (exact mechanism unknown)	
Gpbar1	Tgr5	G-coupled-receptor specific for BA	Unsuccessful
Mucins			
Muc1		Main Mucin, membrane-anchored	
Muc4		Evidence for focal expression in small bile ducts, membrane-anchored	Unsuccessful
Muc20		Expression pattern unknown, membrane-anchored	Unsuccessful

Table S7. Primer Sequences, Related to STAR Methods.

Murine genotyping primer sequences		
Genotype	Direction	Sequence 5' to 3'
Col-YapS127A	Forward (Common)	CCCTCCATGTGTGACCAAGG
	Reverse (Wildtype)	GCACAGCATTGCGGACATGC
	Reverse (Mutant)	GCAGAAGCGCGGCCGTCTGG
Krt19-CreER	Forward (Wildtype)	TCTCGCCTCCTACTTGGACAA
	Forward (Mutant)	CTATCGCCTTCTTGACGAGTT
	Reverse (Common)	ATATCCCTGACTATCCAAGCA
Rosa26-TdTomato (Jax 007909)	Forward (Wildtype)	AAGGGAGCTGCAGTGGAGTA
	Reverse (Wildtype)	CCGAAAATCTGTGGGAAGTC
	Forward (Mutant)	CTGTTCCTGTACGGCATGG
	Reverse (Mutant)	GGCATTAAAGCAGCGTATCC
Rosa26-rtTA	Forward	GGACGAGCTCCACTTAGACG
	Reverse	AGGGCATCGGTAAACATCTG
Cyr61eGFP	Forward	CGACAGAGCTACGTCACTGCAACAC
	Reverse	GGTCGGGGTAGCGGCTGAA
Rosa26	Forward (Wildtype)	GGAGCGGGAGAAATGGATATG
	Forward (Mutant)	AAGACCGCGAAGAGTTTGTC
	Reverse (Common)	AAAGTCGCTCTGAGTTGTTAT
Yapfl/fl	Forward (Common)	AACCACCAAACCTGGCATAG
	Reverse (Wildtype)	GAGGCCAAACCTGACAACTA
	Reverse (Mutant)	GTGCCCAGTCATAGCCGAATA
CAGs-rtTA3	Forward (Common)	AGTCACTTGTCACACAACG
	Reverse (Wildtype)	TGATTATCTGAATTCCTGGGATG
	Reverse (Mutant)	CTCTTATGGAGATCCCTCGAC
Cre	Forward	GCGGTCTGGCAGTAAAAACTATC
	Reverse	GTGAAACAGCATTGCTGTCACTT
Hes1-CreER	Forward	CGTACTGACGGTGGGAGAAT
	Reverse	TGCATGATCTCCGGTATTGA
Rosa26-TdTomato (Jax 007914)	Forward (Wildtype)	AAGGGAGCTGCAGTGGAGTA
	Reverse (Wildtype)	CTTTAAGCCTGCCCAGAAG
	Forward (Mutant)	ACGTCAATAGGGGGCGTACT
Asbt KO	Forward (Wildtype)	CCAGGAAGAGTCAGTGCTCAAAACC
	Forward (Mutant)	GGGATCTCATGCTGGAGTTCTTCG
	Reverse (Common)	TGAAAGATAGAGGGCAGTCAATGATGG
Tgr5 KO	Forward (Common)	GATGCTGGAGCCACTATATCAGGAC
	Reverse (Wildtype)	GACTGCCCTAGAAGGACCCAGAGAC
	Reverse (Mutant)	GGAACAGAGCACTCTGTGACTTCC
Iqgap1 Ko	Forward (Common)	TTGCAGTCTGTGGCATGTG
	Reverse (Wildtype)	CCTGCTGACAGGTCAATGAT
	Reverse (Mutant)	CCTGCTCTTTACTGAAGGCT

Primer sequences used for RT-qPCR analysis

Gene	Direction	Sequence 5' to 3'
Apoc1	Forward	AGAGATCCTTAGATCCAGGGTG
Apoc1	Reverse	TGGCTACGACCACAATCAGG
Cyr61	Forward	AGAGGCTTCCTGTCTTTGGC
Cyr61	Reverse	CCAAGACGTGGTCTGAACGA
Gapdh	Forward	AAGGTCATCCCAGAGCTGAA
Gapdh	Reverse	CTGCTTCACCACCTTCTTGA
Klf6	Forward	GGGAACAGTTTCTGCTCGGA
Klf6	Reverse	CAGGCAGGTCTGTTGCCAAT
Yap1	Forward	CCCTCGTTTTGCCATGAACC
Yap1	Reverse	TCCGTATTGCCTGCCGAAAT
Gadd45b	Forward	CTGATGAATGTGGACCCCGA
Gadd45b	Reverse	CCTCTGCATGCCTGATACCC
Atf3	Forward	CTTCCCCAGTGGAGCCAATC
Atf3	Reverse	TCATTTTGCTCCAGTCTTCGC

Primer sequences used for targeted scRNAseq library amplification

General inDrop forward primer sequence (R1):

5' TCGTCGGCAGCGTCAGATGTGTATAAGAGACAG"gene-specific-sequence" 3'

General inDrop reverse primer sequence (R2):

3' CAAGCAGAAGACGGCATACGAGATGGGTGTCGGGTGCAG 5'

Gene	3' Gene-specific sequences for R1 primer
Slc10a2	5' ACAGCCTGGGTTTCTTCCTG 3'
Slc4a2	5' CTGCTTTGGGCAGTCATGTC 3'
Abcb4	5' GCCGCACCTGCATTGTGATC 3'
Abcb1a	5' ATATGGTGTTTAATCCAAGTC 3'
Slc51a	5' CTGCCAGACCTGGACTCAGC 3'
Slc51b	5' ATCCTGGCAAACAGAAATCG 3'
Abcc3	5' TTCCTTGTCAGATGGACTCG 3'
Iqgap1	5' TGCTTTGGCAGCACCGAGTC 3'
Gpbar1	5' GGCCACATTGCTCCTGTCAG 3'
Muc1	5' CAGCTTTGGCGGTCTGCTC 3'
Muc4	5' GGACCCATCCCTCAGTCTGC 3'
Muc20	5' CCTCTGTGCCAGAAGAACGG 3'